THE JOURNAL OF PHYSICAL CHEMISTRY B

Article

pubs.acs.org/JPCB

Characterization of Agonist Binding to His524 in the Estrogen Receptor α Ligand Binding Domain

Li Gao,[†] Yaoquan Tu,[†] Hans Ågren,*[,†] and Leif A. Eriksson*[,‡]

[†]Division of Theoretical Chemistry and Biology, School of Biotechnology, KTH Royal Institute of Technology, S-106 91 Stockholm, Sweden

[‡]Department of Chemistry and Molecular Biology, University of Gothenburg, 41296 Göteborg, Sweden

Supporting Information

ABSTRACT: The bioactivities of the natural steroidal estrogen 17β-estradiol (E_2), the synthetic estrogen diethylstilbestrol (DES), and the phytoestrogen genistein (GEN) are intimately associated with their binding to the estrogen receptor α ligand binding domain (ERα LBD) and accordingly allostery. Molecular modeling techniques have been performed on agonists in complex with the LBD, focusing on the pivotal role of His524 modeled as the ε-tautomer and the protonated form (depending on pH). It is found that E_2 binds to the active LBD with the aid of Leu525, showing existing stable patterns of an H-binding network with Glu419 via His524 in all models. The main difference seen in the effect is that the full agonists E_2 and DES have higher binding energies to the protonated His524 than the partial agonists GEN and Way-169916 (W), which is in line with noted experimental transcriptional activities. In conclusion, the study demonstrates that the phytoestrogen GEN interacts differently with the LBD than what E_2 and DES do, which explains the observed signaling differences.

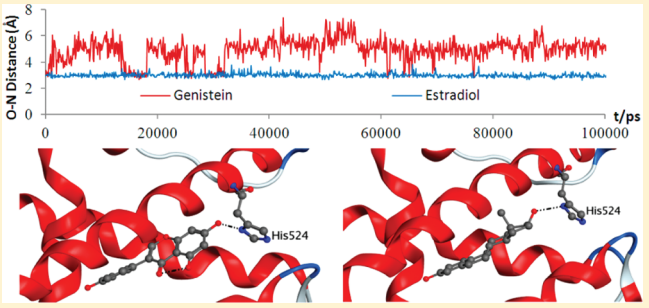

1. INTRODUCTION

Estrogen receptors (ERs) belong to the family of nuclear receptors and modulate transcriptions of target genes in a ligand dependent way, which makes them very attractive drug targets. The endogenous estrogens bind to ERs under physiological conditions, and are associated with a wide range of physiological and pathological pathways.[1−4] The primary female hormone, 17β-estradiol (E_2), is blamed for breast cancer, as it stimulates ER-dependent cancer cell growth; nevertheless, it has also been proven to protect the cardiovascular system, to protect bones against osteoporosis, and to protect the central nervous system against Alzheimer's disease.[5−9] There are several exogenous compounds that, albeit structurally very different from the steroid hormones, possess full or partial estrogenic activity.[10] Diethylstilbestrol (DES) is the most infamous potent synthetic estrogen, and has been withdrawn from use in pregnant women. Exposure to DES is associated with many adverse health consequences,[11,12] such as development of a rare vaginal tumor and an increased risk of breast cancer.[13,14] In contrast, the principal phytoestrogen genistein (GEN), found in soy, appears to reduce the risk of breast cancer.[15] The historically low breast cancer prevalence in Asia is ascribed to consumption of soyfood in these countries.[16] However, the conclusions are not in consensus, as GEN has estrogen-like effects under some experimental conditions and stimulates ER-positive breast cancer cell growth.[17,18] Compared to GEN, the compound Way-169916 (W) is a less potent partial agonist that works through an ER-dependent mechanism. It exerts broad anti-inflammatory activity *in vivo* but is devoid of conventional estrogenic action, associated with strong transcriptional activation, i.e., proliferative effects.[19−21] However, little is known about what governs the regular biological activity, or modulates transcription response.

The ER ligands bind to the ligand binding domain (LBD) and induce conformational changes, mainly of the flexible C-terminal helix 12 (H12). The apo conformation of the unbound LBD is assumed to orient with the solvent exposed H12 extended away from the protein.[22] The endogenous or exogenous ligands are captured in the binding site region. As a ligand is introduced, the apo-LBD is rearranged into a closed/agonist−LBD or an open/antagonist−LBD, which affects the subsequent recruitment of different coregulators for the activation or silencing of ERs.[23,24] Numerous studies have focused on the LBD of ERs, and about 100 cocrystallized ligand−LBD structures have been solved and deposited in the RCSB Protein Data Bank (PDB). The generally classified agonist or antagonist LBD conformers refer to the positioning of H12 but not to the detailed folding process and the resulting bioactivity which is subtly influenced by individual ligands. Understanding the ligand induced allostery is important for clarifying how small molecules regulate physiological functions and for developing improved therapeutic agents.

Received: January 27, 2012
Revised: April 3, 2012
Published: April 7, 2012

   dx.doi.org/10.1021/jp300895g | J. Phys. Chem. B 2012, 116, 4823−4830

The ERα ligands discussed herein, E_2, DES, GEN, and W, are classified as full or partial agonists and stabilize H12 in the agonist conformation. The agonists bind to the LBD through H-bonding and van der Waals contacts. Besides the hydrophobic features of the pocket, ligands with a high affinity to ERα usually form H-bonds with primarily the side chains of Glu353, Arg394, and His524, as illustrated with the E_2−LBD complex in Figure 1. His524 stands a pivotal role in maintaining

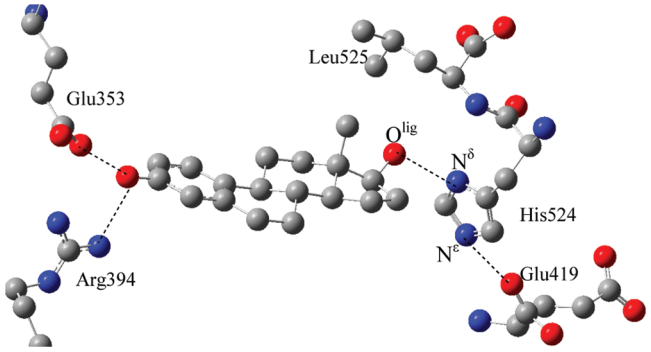

Figure 1. Representation of the ligand binding in the agonist-ERα LBD form. E_2 is used to illustrate how the agonist forms contacts with the receptor; PDB code 1g50.[25]

the protein structure in the agonist−LBD conformer, where a conserved H-bonding network is found from the ligand to the Glu419 backbone via the His524 side chain, i.e., $O^{lig}\cdots N^{\delta}$(His524)$N^{\varepsilon}\cdots O{=}C$(Glu419), and is ascribed to the versatile imidazole ring. Both His524 and Leu525 are geometrically in contact with the agonist ligands in the crystal structures, and are furthermore located on H11, which is closely linked to the essential H12. Hence, His524 and Leu525 are involved in ligand binding and allostery, which are intimately involved in the transcriptional activation of ERα agonists. Experimentally, mutations of either amino acids His524 or Leu525 to alanine results in large reductions in agonist-induced transcriptional response and binding affinity, with the pattern differing depending on the activating ligand.[26,27]

It is the objective of this study to investigate the influence of the agonist ligand on the interaction strength that gives rise to the most stable binding pattern to His524 and Leu525, of importance for understanding small-molecule signaling through ERα. For this purpose, DFT calculations and molecular dynamics (MD) simulations are performed in order to obtain information about agonists bound to His524 and Leu525, and the features of their dynamical behavior upon changes in pH. Special attention is paid to the H-binding of specific tautomers and protonated forms of the imidazole side chain of His524.

2. MATERIALS AND METHODS

To describe the noncovalent interactions between agonists and ERα LBD, the highly parametrized exchange-correlation functional M06-2X[28,29] was used, which has been proven to provide reliable results for dispersive interactions.[30,31] All DFT-based calculations were performed using the Gaussian 09 program package[32] at the M06-2X/6-31+G(d,p) level of theory, as a good compromise between accuracy and computational cost.[33] Initial coordinates of the E_2−His524(Leu525)−Glu419 complex were extracted from the cocrystallized E_2 and human ERα LBD X-ray structure with PDB code 1g50,[25] and for DES, GEN, and W complexes from 3erd,[23] 1x7r,[34] and 2qzo,[35] respectively. Geometry optimizations were carried out *in vacuo* for all systems. Bulk solvation effects were considered through single-point calculations using the integral equation formalism variant of the polarized continuum model (IEFPCM)[36−39] with default parameters. To model the water and protein surroundings, the dielectric constants 78.36 and 4.24 were used, respectively. Harmonic vibrational frequency calculations were performed in vacuum (ε = 1), hydrophobic environment (ε = 4.24), and water (ε = 78.36) to extract zero point corrections. In the ligand binding pocket model, some centers were held fixed to their X-ray positions in the geometry optimization steps, such as the truncated termini or atoms that interact with other parts of the receptor. The binding energies with ZPE-corrections are calculated as

$$\Delta\Delta E_{\text{binding}} = \Delta E_{\text{total}} - \Delta E_{\text{ligand}} - \Delta E_{\text{residues}}$$

MD simulations were performed for E_2−LBD and GEN−LBD complexes to compare the dynamic behavior of a full agonist and a partial agonist contacting the LBD. The X-ray structure 1g50 used in DFT calculations of E_2−LBD was used as a starting point. For GEN−LBD, since the PDB structure 1x7r is not completely modeled, the starting geometry was created by replacing E_2 in 1g50 by GEN according to its positioning in 1x7r. Independent MD simulations were conducted for each system at pH 6.5 and pH 7.5 to mimic the corresponding protonated and neutral His524 as outlined below. The ligand−LBD complex was solvated in a periodic box with TIP3P[40] water molecules extending 10 Å outside the protein, giving a total of 30332−30352 atoms. 100 ns of unrestrained MD simulations were carried out at 298 K using the program YASARA structure,[41] after initial energy minimization procedures. The AMBER03[42] force field was used for the protein and the general Amber force field[43] (GAFF) for the ligands. All systems were neutralized,[44] and additional Na^+ or Cl^- were added to give a total NaCl concentration of 0.9%. Particle-mesh Ewald (PME) summation for the electrostatics was used for long-range Coulomb interactions with a cutoff of 7.86 Å. The complete processes were carried out using a predefined macro (run_md) within the YASARA package.

3. RESULTS AND DISCUSSION

3.1. H-Binding between Ligand and His524. All ligands discussed in the current work are shown in Scheme 1. Each ligand has a phenolic hydroxyl group in the *para* position, which anchors the ligand to the binding pocket through two H-bonds with Glu353 and Arg394, respectively. This interaction between ligand and receptor is in consensus for the four molecules and is thus not discussed further herein. Special attention is instead paid to the H-bonds between His524 and the hydroxyl groups of E_2, DES, and GEN, and the CF_3 group of W, which are oriented toward the imidazole ring of His524, as shown in Figure 2.

Construction of a H-bond requires the presence of a partially positive H atom from the donor to interact with the H-bond receptor, normally a nonbonding electron pair of a heteroatom. In the current cases of E_2, DES, and GEN, the hydroxyl group interacting with His524 may serve as either a H-bond donator via its hydrogen atom or a H-bond acceptor to one of the lone pairs of the hydroxyl oxygen, depending on the protonation state of the histidine. Hence, the nature of the H-bond will depend on both the characteristics of the hydroxyl group of the ligand and on the His524 state.

dx.doi.org/10.1021/jp300895g | J. Phys. Chem. B 2012, 116, 4823−4830

Scheme 1. Structures of ERα Ligands Studied Herein[a]

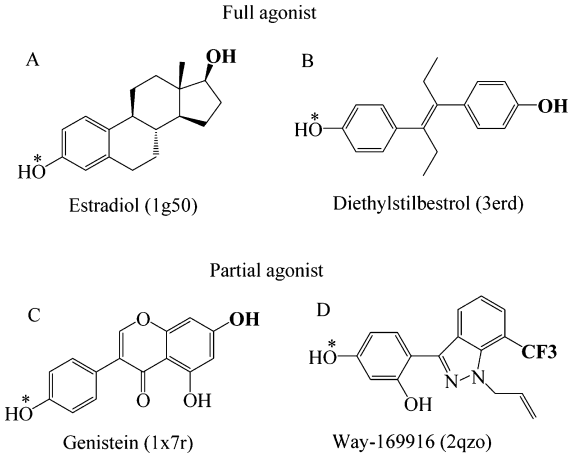

[a]Full agonists: (A) 17β-estradiol (E_2, a natural estrogen); (B) diethystilbestrol (DES, a synthetic estrogen). Partial agonists: (C) genistein (GEN, a phytoestrogen); (D) Way-169916 (W, a pathway-selective ER ligand). Asterisks indicate the hydroxyl groups that are bound to Glu353 and Arg394 of ERα in the cocrystallized structures, and the groups in boldface are coordinated to His524. PDB codes are reported in parentheses.

Hydroxyl Group. Hydrogen bond formation can be related to proton affinities of the acceptor/deprotonation energies of the donor. In the case of the hydroxyl group coordinated to His524, the deprotonation energies and proton affinities are compared for E_2, DES, and GEN in vacuum ($\varepsilon = 1$), water ($\varepsilon = 78.36$), and the hydrophobic medium ($\varepsilon = 4.24$) to model the protein environment. The results shown in Table 1 indicate that the more polar the medium is, the more the deprotonation energies decrease and the proton affinities increase, as a result of the enhanced stabilization of the charged species. The aliphatic hydroxyl group of E_2 has the highest deprotonation energies and proton affinities in all models, indicating that it is less likely to function as a H-bond donor; accordingly, it is more prone to accept a proton and work as a H-bond acceptor. Conversely, the phenolic hydroxyl group of GEN has the lowest deprotonation energies and proton affinities; 18−39 kcal/mol less than those of E_2. The energy difference thus indicates that GEN is more prone to share the H atom with the H-bond acceptor, and correspondingly that it also works as a less potent H-bond acceptor. For DES, the analogous phenolic hydroxyl group has both medium deprotonation energies and proton affinities. It may thus be expected to function as either a H-bond donor or acceptor, depending on the protonation state of the associated His524.

Table 1. ZPE-Corrected Deprotonation Energies and Proton Affinities for Each Ligand (in kcal/mol) of the Hydroxy Groups Which Binds to His524, as Shown in Figure 2

	$\varepsilon = 1$	$\varepsilon = 4.24$	$\varepsilon = 78.36$
	Deprotonation Energies		
E_2	365.9	326.2	312.2
DES	341.2	305.9	293.9
GEN	327.0	294.8	284.6
	Proton Affinities		
E_2	193.4	230.7	242.5
DES	180.2	218.9	230.8
GEN	172.6	211.8	224.1

His524. The imidazole ring of His is chemically versatile and includes three distinct forms, i.e., two neutral forms, referred to as ε-tautomer (N^{ε}—H) and δ-tautomer (N^{δ}—H), and a

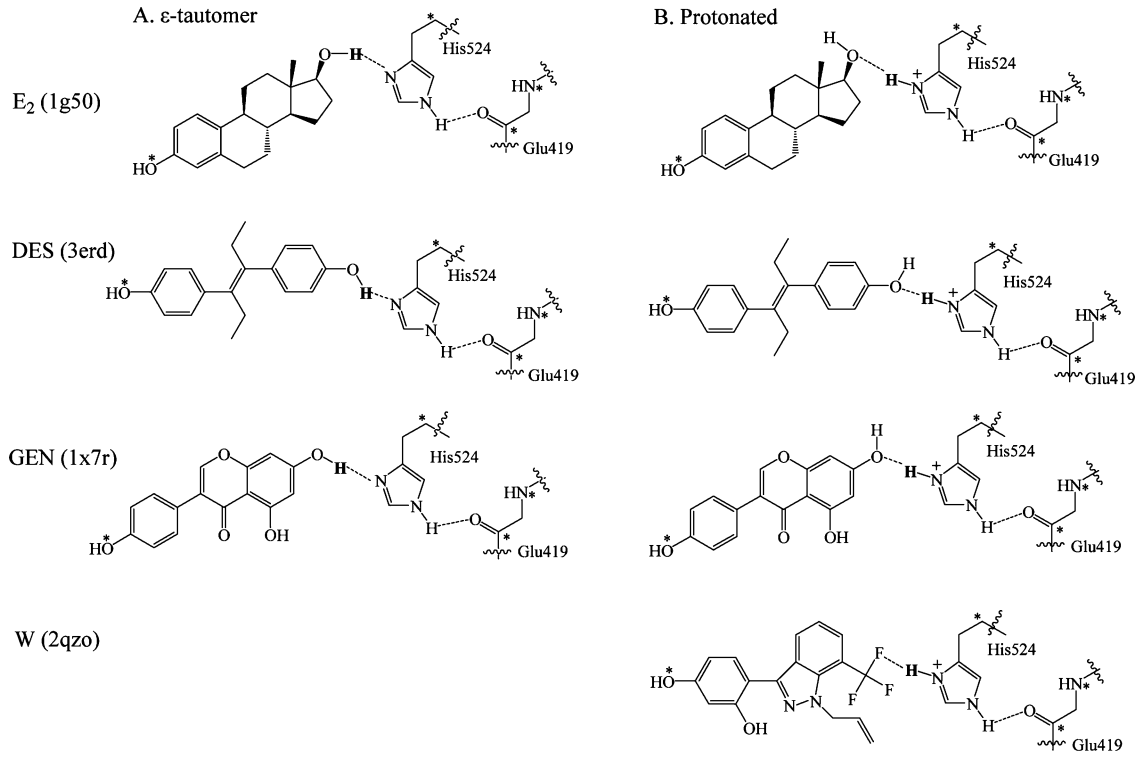

Figure 2. The schematic structures of systems modeled for the ligand···His524···Glu419 H-bonding network. Asterisks indicate the atoms that are fixed to their X-ray positions in the geometry optimization steps.

dx.doi.org/10.1021/jp300895g | J. Phys. Chem. B 2012, 116, 4823−4830

positively charged, protonated form, as seen in Scheme 2. In the cocrystallized structures of the ligand in complex with

Scheme 2. Side Chain of Histidine in Different States and Tautomers

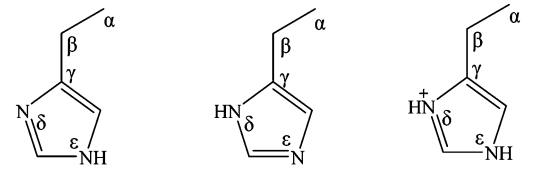

A. ε-tautomer B. δ-tautomer C. Protonated

agonist−LBD, conserved distances of 2.9−3.1 Å were found between N^{ε}(His524) and the carbonyl oxygen of the Glu419 backbone. The X-ray data indicates that the N^{ε}—H is required to form a conserved H-bonding between His524 and the Glu419 backbone (N^{ε}—H···O═C). Hence, the possible forms of the imidazole ring are either the ε-tautomer or the protonated form. The ε-tautomer forms a H-bond to the ligand, O—H^{lig}···N^{δ}(His524), whereby the hydroxyl group of the ligand acts as a proton donor interacting with the electrons from the N^{δ}(His524) lone pair (Figure 2A). Another possibility is that the protonated imidazole ring functions as a donor and forms a H-bond with the electrons from the O^{lig} lone pair, O^{lig}···H−N^{δ}(His524), as seen in Figure 2B.

H-Binding. The X-ray diffraction data available for the solved protein crystals do not display the explicit hydrogen atoms. In the current cases, the distances of 2.6−2.7 Å between O^{lig} and N^{δ}(His524) only suggest the existence of a H-bonding interaction but not the direction thereof. It is difficult to determine whether the imidazole ring of His524 is in the ε-tautomer or the protonated form, since the imidazole states may vary significantly with the environment, affected by the agonist ligand and the allostery effect going from the apo- to the agonist−LBD conformation. To establish possible H-bonding models, hydrogen atoms were added to the system using force field methods and modified manually to position as indicated by the X-ray diffraction data. The binding energies between E_2/DES/GEN and His524 were calculated for both the ε-tautomer and the protonated His524, respectively. For W in complex with the LBD, the shortest distance between the $-CF_3$ group and N^{δ}(His524) is 3.4 Å. An attractive interaction is only possible when the protonated imidazole ring functions as a proton donor with N^{δ}−H coordinated to the electron lone pair of an F atom. All systems modeled are depicted in Figure 2.

The binding energies of ligands to His524 thus obtained are shown in Table 2 for both the ε-tautomer and the protonated

Table 2. ZPE-Corrected Binding Energies (in kcal/mol) of Ligand Bound to His524 as Shown in Figure 2

	ε = 1	ε = 4.24	ε = 78.36
	ε-Tautomer O−H^{lig}···N^{δ}(His524)		
E_2	6.63	5.35	4.64
DES	13.32	11.46	10.42
GEN	14.71	12.60	11.46
	Protonated O^{lig}···H−N^{δ}(His524)		
E_2	17.58	9.50	6.83
DES	13.95	7.46	5.57
GEN	11.34	5.48	3.82
W	7.82	−0.30	0.01

imidazole ring mediated H-bond network. In general, the bond strength is weaker in the more polar medium due to the corresponding reduction of electrostatic interactions, and this effect is significant in the systems with the charged His524. Of the specified hydroxyl group of ligands discussed herein, E_2 is the best hydrogen bond acceptor and GEN the best hydrogen bond donor, as suggested by the proton affinities and deprotonation energies (Table 1). The binding energies obtained (Table 2) are consistent with these findings. E_2 has the highest binding energies (6.83−17.58 kcal/mol) to the protonated His524, O^{lig}···H−N^{δ}(His524), in which the ligand functions as a hydrogen bond acceptor, while GEN has the highest binding energies (11.46−14.71 kcal/mol) to the ε-tautomer, O−H^{lig}···N^{δ}(His524), in which the ligand functions as a hydrogen bond acceptor. DES has intermediate binding energies in all models, while W interacts weakly with His524, which agrees well with its lower potency compared to, e.g., GEN.[19−21]

3.2. Ligand in Contact with His524 and Leu525. Since experiments have proven that both His524 and Leu525 are involved in the bioactivity of agonists,[26,27] the models were extended to identify the agonist binding strength to these two amino acids. The modeled systems and their optimized structures are shown in Figure 3 and Figure S1 in the Supporting Information, with geometrical parameters of the H-bonding network displayed in Table 3. In the optimized structures, the distances between the H-bond donor and the corresponding acceptor (d O^{lig}−N^{δ} and d N^{ε}−O^{glu}) are comparable to their X-ray structures for all models, which indicate the possibility of both H-bonding patterns. However, the angles for the H-bonds vary significantly mainly due to the restriction in possible orientations imposed by the protein environment, modeled indirectly by fixing selected atoms in the optimization steps.

Binding energies thus obtained are given in Table 4; they are found to be of comparable magnitude to those of binding to His524 only, Table 2. The binding energies are generally increased by ∼0−3 kcal/mol with the inclusion of Leu525, depending on the ligand, except E_2 bound to the ε-tautomer of His524, in which case the binding energies increased by ∼6 kcal/mol. The optimized structure of the E_2 complex shown in Figure 3A reveals that the H atom of the hydroxyl group is positioned toward N^{δ}, whereby the O atom is exposed to the side chain of Leu525 which facilitates the interaction between E_2 and Leu525. E_2 has the lowest binding energy as the hydrogen bond donor in the His524 ε-tautomer only model (Table 2), but the interaction with Leu525 is highly favorable and compensates to the total binding to the receptor. E_2, DES, and GEN all have sufficiently high binding energies to the LBD in the ε-tautomer models. In contrast to E_2, Leu525 does not contribute significantly toward the binding of GEN and W. In the protonated models, the partial agonists GEN and W have much lower binding energies than the full agonists E_2 and DES. These results are in good agreement with the experimental binding affinities and bioactivity trends. Both the natural E_2 and the synthetic estrogen DES have potent transcriptional activities with equivalent binding affinity to ERα, which in turn is ∼70-fold higher than GEN.[45,46] W is observed experimentally to have a 433-fold lower binding affinity than E_2 to ERα, and shows no ER-dependent transcriptional activity.[21]

3.3. MD Simulations of E_2−LBD and GEN−LBD Complexes. Unrestrained all-atom molecular dynamics

dx.doi.org/10.1021/jp300895g | J. Phys. Chem. B 2012, 116, 4823−4830

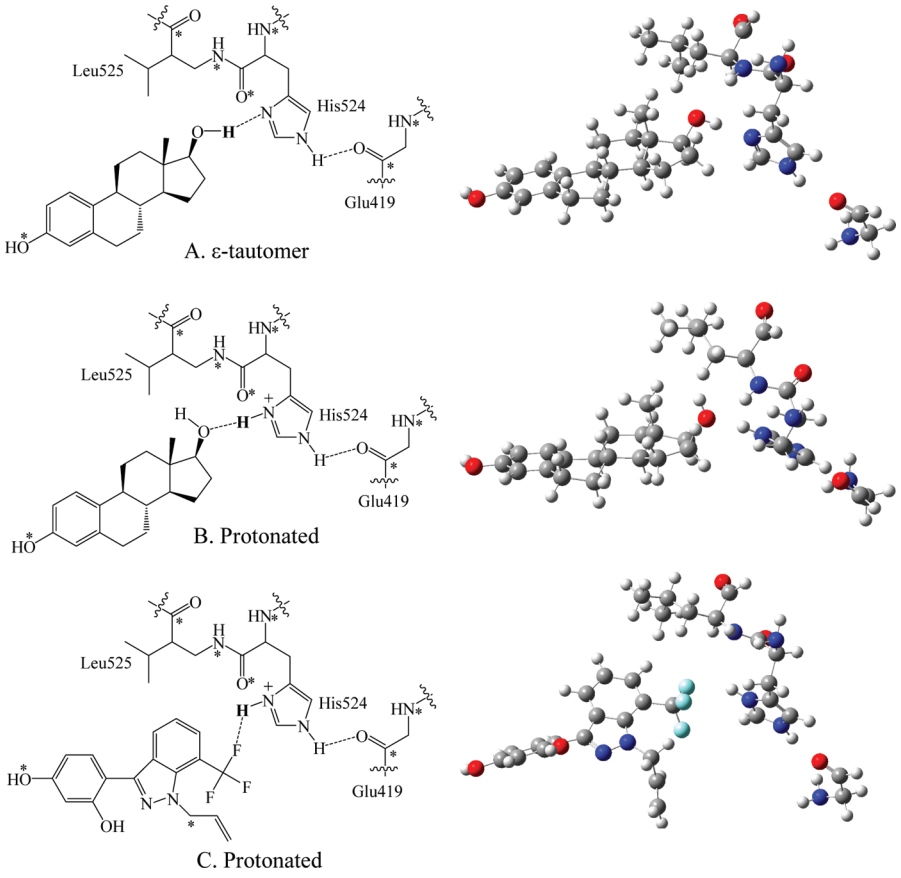

Figure 3. Schematic and optimized structures of systems modeled for ligand and part of the binding region of ERα LBD. Asterisks indicate the atoms that are fixed to their X-ray positions in the geometry optimization steps. (A) E_2 bound to the neutral His524 in its ε-tautomer. (B) E_2 bound to the protonated His524. (C) W bound to the protonated His524.

Table 3. Selected Geometrical Parameters for the H-Binding Network Optimized at the M062X/6-31+G(d,p) Level of Theory in Vacuo[a]

	O—H^{lig}···N^{δ}(His524)			(His524)N^{ε}—H···O=C(Glu419)		
ε-tautomer	d O^{lig}—N^{δ}	d H^{lig}—N^{δ}	∠O—H^{lig}···N^{δ}	d Nε—O^{glu}	d $H^{N\varepsilon}$—O^{glu}	∠N^{ε}—H···O^{glu}
E_2	2.833(2.7)	1.859	169.8	2.906(3.0)	2.056	140.0
DES	2.716(2.6)	1.769	158.5	2.923(2.9)	1.914	171.8
GEN	2.654(2.6)	1.644	177.1	2.907(2.9)	1.898	172.1
	O^{lig}···H—N^{δ}(His524)			(His524)N^{ε}—H···O=C(Glu419)		
protonated	d O^{lig}—N^{δ}	d O^{lig}—$H^{N\delta}$	∠O^{lig}···H—N^{δ}	d N^{ε}—O^{glu}	d $H^{N\varepsilon}$—O^{glu}	∠N^{ε}—H···O^{glu}
E_2	2.759(2.7)	1.744	163.9	2.781(3.0)	1.897	142.9
DES	2.815(2.6)	1.890	148.3	2.709(2.9)	1.685	169.8
GEN	2.812(2.6)	1.793	169.9	2.687(2.9)	1.655	173.4
W[b]	3.358(3.4)	2.452	148.0	2.809(3.1)	1.837	156.8

[a]The systems modeled are shown in Figure 3 and Figure S1 in the Supporting Information. O^{lig} and H^{lig} correspond to the hydroxyl group interacting with His524 of each ligand (experimental data in parentheses[23,25,34,35]). [b]The geometries in each terms correspond to the F^{lig} atom of the $-CF_3$ group instead of the O^{lig} atom of other ligands.

(MD) simulations were conducted of the E_2−LBD and GEN−LBD systems in explicit water. The focus is on describing the H-bonding network of ligand···His524···Glu419 upon pH changes for the full agonist E_2 and the partial agonist GEN. The histidine is expected to be neutral at high pH, i.e., the ε-tautomer His524 in the current study, due to the requirement of H-bonding between the N^{ε}−H proton and the carbonyl group of the Glu419 backbone. Protonated histidines are commonly found at neutral and acidic pH. The N^{ε}−H and N^{δ}−H protons of the protonated imidazole ring on His524 enable this to form two H-bonds as a donor, to the ligand and Glu419, respectively. To explore both possibilities, simulations at pH 7.5 were carried out to model the ligand−LBD for the ε-tautomer His524, and the system with protonated His524 was modeled through simulations at pH 6.5.

In Figure 4, plots of key distances and angles of the H-binding network are displayed for the complete trajectories of the 100 ns MD simulations. For the ε-tautomer of His524 at pH 7.5, the distances and corresponding hydrogen bond angles are plotted for the H-bonding mode, O^{lig}—H···N^{δ}(His524)-

dx.doi.org/10.1021/jp300895g | J. Phys. Chem. B 2012, 116, 4823−4830

Table 4. ZPE-Corrected Binding Energies (in kcal/mol) of Ligand Bound to His524 and Leu525 as Shown in Figure 3 and Figure S1 in the Supporting Information

	ε = 1	ε = 4.24	ε = 78.36
	ε-Tautomer O–H^{lig}···N$^{\delta}$(His524)–Leu525		
E_2	13.53	11.47	10.32
DES	16.38	13.77	12.69
GEN	16.77	14.05	12.26
	Protonated O^{lig}···H–N$^{\delta}$(His524)–Leu525		
E_2	18.92	10.66	7.90
DES	16.66	10.61	8.72
GEN	12.06	5.82	2.79
W	7.55	2.68	1.33

N$^{\varepsilon}$—H···O=C(Glu419), of the E_2–LBD and GEN–LBD systems in Figure 4A and B, respectively. In both systems, the H-bonding network is conserved throughout the simulations, with distances stabilized around 3 Å for the centers of the two individual H-bonds, i.e., distances between O^{lig} and N$^{\delta}$ and between N$^{\varepsilon}$ and O^{glu}. The corresponding angles of the hydrogen bonds are generally stable, although with some fluctuations. For the protonated His524 at pH 6.5, the corresponding geometrical parameters are plotted for the H-binding mode, O^{lig}···H—N$^{\delta}$(His524)N$^{\varepsilon}$—H···O=C(Glu419) of the E_2–LBD and GEN–LBD systems in Figure 4C and D, respectively. In this protonation state, a conserved H-bonding network is only found in the E_2–LBD system, with distances and angles analogous to those found for the ε-tautomer of His524 in the high pH environment. However, the partial agonist GEN is not able to retain the conserved network observed in the agonist–LBD X-ray crystal structures, when His524 is assumed to be protonated. Indeed, partial agonists were experimentally proven difficult to cocrystallize with LBD, which has been ascribed to the possible reason that it may communicate the LBD with mixed active and inactive conformations.[35] Mutation techniques were thus used to aid the cocrystallization of GEN and other partial agonists with the LBD.[34,35]

The full agonist E_2 binds the ERα LBD in an optimal manner and stabilizes the conserved H-binding network with Glu419 via His524 in the active agonist–LBD conformation under all conditions discussed herein. The partial agonist GEN mimics the actions of E_2 in the ε-tautomer model of His524 but does not interact strongly in the case of protonated His524. Hence, we conclude that GEN does not function as a full agonist under physiological conditions as the natural or synthetic estrogens do. Experimentally, the interactions between the ligand and His524 have proven important for the estrogenic actions of agonists, through mutation of His524 to alanine.[26,27] In addition, alkyl substitution of the ligand hydroxyl group blocks the interaction with His524, and transforms the estrogenic ligands into antiestrogenic ones.[47] Furthermore, GEN has proven experimentally to block the gene expression which is stimulated by E_2.[48]

Worth noting is that hydrogen atoms should be added with care to the system in the starting point, in order to enable the appropriate connections between ligands and His524 for both the ε-tautomer and the protonated form. Otherwise, neither the DFT geometry optimization steps nor the force field simulations are able to flip the hydrogen atom of the hydroxyl

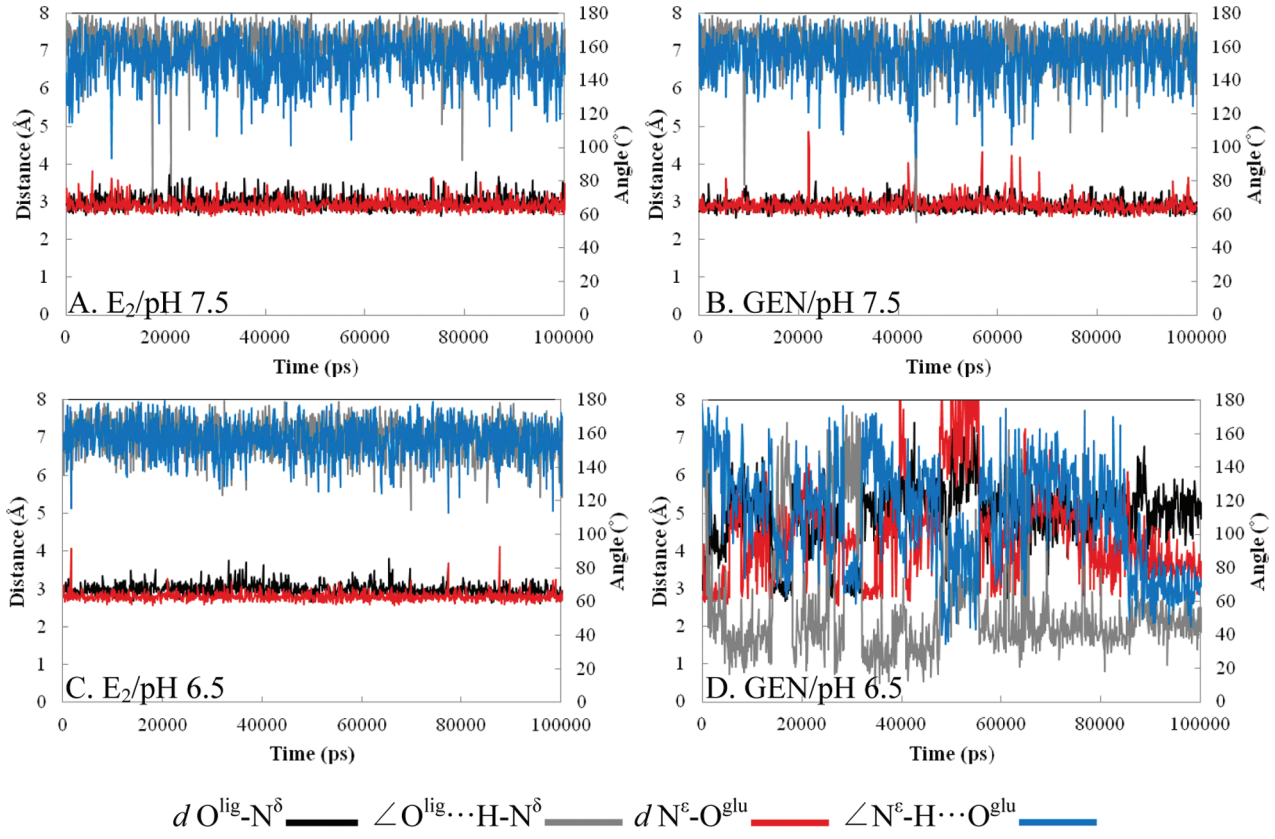

Figure 4. H-bond distances and corresponding angles of (E_2)O···N$^{\delta}$(His524)N$^{\varepsilon}$···O=C(Glu419) at (A) pH 7.5 and (C) pH 6.5 and those of (GEN)O···N$^{\delta}$(His524)N$^{\varepsilon}$···O=C(Glu419) at (B) pH 7.5 and (D) pH 6.5.

dx.doi.org/10.1021/jp300895g | J. Phys. Chem. B 2012, 116, 4823–4830

group to the right position to allow for appropriate H-bonding to His524, as depicted in Figure 2.

4. CONCLUSIONS

With the aid of mutation techniques, partial agonists have been cocrystallized with ERα LBD, stabilizing H12 in the canonical agonist−LBD conformation in the same manner as full agonists. The bioactivity of ERα is thus adjusted by small molecules via ligand-induced allostery, whereby the process of H12 folding to the agonist or antagonist conformation is subtly affected by ligands. We have herein performed DFT calculations and forced field based MD simulations on full and partial agonists in complex with LBD, which allowed for a better understanding of the possible interactions between ligand and the conformationally active agonist−LBD. The binding strength to His524−Leu525 and corresponding estrogenic potency are discussed in terms of the calculated binding energies and H-bonding patterns with regard to the tautomer and charge of His524.

The ε-tautomer and the protonated imidazole ring of His524 are used in the models of the natural steroidal estrogen E_2, the synthetic estrogen DES, the phytoestrogen GEN, and the pathway-dependent partial agonist W, bound to the agonist−LBD. The aliphatic hydroxyl group of E_2 has the highest proton affinity and deprotonation energy of E_2, DES, and GEN, consistent with trends in H-bond strength to His524, i.e., high affinity to the protonated His524 ($O^{lig}\cdots H—N^{\delta}$), thereby acting as a good hydrogen bond acceptor; low affinity to the ε-tautomer ($O^{lig}—H\cdots N^{\delta}$) and is thus a poor hydrogen bond donor. However, E_2 stabilizes the ε-tautomer $O^{lig}—H\cdots N^{\delta}(His524)N^{\varepsilon}—H\cdots O{=}C(Glu419)$ network due to an optimum interaction with Leu525, which contributes ∼6 kcal/mol extra to the binding energy. Conversely, the phenolic hydroxyl group of GEN has the lowest proton affinity and deprotonation energy, which corresponds to a low affinity to the protonated His524, and that it cannot stabilize the $O^{lig}\cdots H—N^{\delta}(His524)N^{\varepsilon}—H\cdots O{=}C(Glu419)$ network, as Leu525 does not contribute to the GEN binding. MD simulations were conducted, focusing on the effects of the ligand on the H-binding network. The results show that E_2 stabilizes the H-binding network with Glu419 via His524 in all models, while the effects of GEN highly depend on the protonation state of His524, giving a stable structure at pH 7.5 and an unstable structure at pH 6.5. The computational results are in good agreement with the experimental observations and bioactivities, explaining why the partial agonist GEN is hard to cocrystallize with LBD, and displays less estrogenic activity than the full agonist. For the fairly weak partial agonist W, the estimated binding energies to His524 and Leu525 are much weaker than what was found for the other ligands, which is also in good agreement with the experimental findings.

The occurrence of the principal phytoestrogen GEN in soyfood is highly correlated to the observed low breast cancer prevalence in Asian countries. An obstacle to the further use of GEN is that it is also observed to stimulate ER-positive breast cancer cell growth. Further research is needed to delicately balance the antiestrogen and estrogenic properties of such agonist-like ligands, as these may provide a better choice than the antagonist-like compounds in the prevention of breast cancer. This is because of the common side effects of antagonists such as menopause symptoms when deprived of estrogens, commonly observed for patients treated with tamoxifen or raloxifene.[49,50]

■ ASSOCIATED CONTENT

Supporting Information

The schematic and optimized structures of systems modeled for DES and GEN in complex with part of the binding region of ERα LBD. This material is available free of charge via the Internet at http://pubs.acs.org.

■ AUTHOR INFORMATION

Corresponding Author

*E-mail: agren@theochem.kth.se (H.A.); leif.eriksson@chem.gu.se (L.A.E.).

Notes

The authors declare no competing financial interest.

■ ACKNOWLEDGMENTS

We are grateful for grants of computing time from the Swedish National Infrastructure for Computing (SNIC) for the project "Multiphysics Modeling of Molecular Materials", SNIC 022/09-25. The faculty of science at University of Gothenburg and the Swedish Science Council (VR) are gratefully acknowledged for financial support.

■ REFERENCES

(1) Korach, K. S.; Hewitt, S. C.; Couse, J. F. *Breast Cancer Res.* **2000**, *2*, 345−352.
(2) Ettinger, B. *Proc. Soc. Exp. Biol. Med.* **1998**, *217*, 2−5.
(3) Korach, K. S.; Deroo, B. J. *J. Clin. Invest.* **2006**, *116*, 561−570.
(4) Gustafsson, J. A.; Heldring, N.; Pike, A.; Andersson, S.; Matthews, J.; Cheng, G.; Hartman, J.; Tujague, M.; Strom, A.; Treuter, E.; Warner, M. *Physiol. Rev.* **2007**, *87*, 905−931.
(5) Mendelsohn, M. E.; Karas, R. H. *Science* **2005**, *308*, 1583−1587.
(6) Cauley, J. A.; Seeley, D. G.; Ensrud, K.; Ettinger, B.; Black, D.; Cummings, S. R. *Ann. Intern. Med.* **1995**, *122*, 9−16.
(7) Mora, S.; Kershner, D. W.; Vigilance, C. P.; Blumenthal, R. S. *Curr. Treat. Options Cardiovasc. Med.* **2001**, *3*, 67−79.
(8) Riggs, B. L.; Khosla, S.; Melton, L. J. *Endocr. Rev.* **2002**, *23*, 279−302.
(9) Sherwin, B. B. *Trends Pharmacol. Sci.* **2002**, *23*, 527−534.
(10) Diamanti-Kandarakis, E.; Bourguignon, J. P.; Giudice, L. C.; Hauser, R.; Prins, G. S.; Soto, A. M.; Zoeller, R. T.; Gore, A. C. *Endocr. Rev.* **2009**, *30*, 293−342.
(11) O'Reilly, E. J.; Mirzaei, F.; Forman, M. R.; Ascherio, A. *Am. J. Epidemiol.* **2010**, *171*, 876−882.
(12) Giusti, R. M.; Iwamoto, K.; Hatch, E. E. *Ann. Intern. Med.* **1995**, *122*, 778−788.
(13) Herbst, A. L.; Ulfelder, H.; Poskanzer, D. C. *N. Engl. J. Med.* **1971**, *284*, 878−881.
(14) Palmer, J. R.; Hatch, E. E.; Rosenberg, C. L.; Hartge, P.; Kaufman, R. H.; Titus-Ernstoff, L.; Noller, K. L.; Herbst, A. L.; Rao, R. S.; Troisi, R.; Colton, T.; Hoover, R. N. *Cancer Cause. Control* **2002**, *13*, 753−758.
(15) Warri, A.; Saarinen, N.; Makela, S.; Hilakivi-Clarke, L. *Br. J. Cancer* **2008**, *98*, 1485−1493.
(16) Messina, M. J.; Persky, V.; Setchell, K. D. R.; Barnes, S. *Nutr. Cancer* **1994**, *21*, 113−131.
(17) Matsumura, A.; Ghosh, A.; Pope, G. S.; Darbre, P. D. *J. Steroid Biochem. Mol. Biol.* **2005**, *94*, 431−443.
(18) Ju, Y. H.; Allred, K. F.; Allred, C. D.; Helferich, W. G. *Carcinogenesis* **2006**, *27*, 1292−1299.
(19) Booth, E. A.; Marchesi, M.; Knittel, A. K.; Kilbourne, E. J.; Lucchesi, B. R. *J. Cardiovasc. Pharmacol.* **2007**, *49*, 401−407.
(20) Keith, J. C.; Albert, L. M.; Leathurby, Y.; Follettie, M.; Wang, L. L.; Borges-Marcucci, L.; Chadwick, C. C.; Steffan, R. J.; Harnish, D. C. *Arthritis Res. Ther.* **2005**, *7*, R427−R438.
(21) Chadwick, C. C.; Chippari, S.; Matelan, E.; Borges-Marcucci, L.; Eckert, A. M.; Keith, J. C., Jr.; Albert, L. M.; Leathurby, Y.; Harris, H.

A.; Bhat, R. A.; et al. *Proc. Natl. Acad. Sci. U.S.A.* **2005**, *102*, 2543−2548.
(22) Sigler, P. B.; Tanenbaum, D. M.; Wang, Y.; Williams, S. P. *Proc. Natl. Acad. Sci. U.S.A.* **1998**, *95*, 5998−6003.
(23) Shiau, A. K.; Barstad, D.; Loria, P. M.; Cheng, L.; Kushner, P. J.; Agard, D. A.; Greene, G. L. *Cell* **1998**, *95*, 927−937.
(24) Brzozowski, A. M.; Pike, A. C.; Dauter, Z.; Hubbard, R. E.; Bonn, T.; Engstrom, O.; Ohman, L.; Greene, G. L.; Gustafsson, J. A.; Carlquist, M. *Nature* **1997**, *389*, 753−758.
(25) Eiler, S.; Gangloff, M.; Duclaud, S.; Moras, D.; Ruff, M. *Protein Expression Purif.* **2001**, *22*, 165−173.
(26) Ekena, K.; Weis, K. E.; Katzenellenbogen, J. A.; Katzenellenbogen, B. S. *J. Biol. Chem.* **1997**, *272*, 5069−5075.
(27) Ekena, K.; Weis, K. E.; Katzenellenbogen, J. A.; Katzenellenbogen, B. S. *J. Biol. Chem.* **1996**, *271*, 20053−20059.
(28) Zhao, Y.; Truhlar, D. G. *Theor. Chem. Acc.* **2008**, *120*, 215−241.
(29) Zhao, Y.; Truhlar, D. G. *Acc. Chem. Res.* **2008**, *41*, 157−167.
(30) Baldridge, K. K.; Peverati, R. *J. Chem. Theory Comput.* **2008**, *4*, 2030−2048.
(31) Lill, S. O. N. *J. Phys. Chem. A* **2009**, *113*, 10321−10326.
(32) Frisch, M. J.; Trucks, G. W.; Schlegel, H. B.; Scuseria, G. E.; Robb, M. A.; Cheeseman, J. R.; Scalmani, G.; Barone, V.; Mennucci, B.; Petersson, G. A.; et al. Gaussian, Inc.: Wallingford, CT, 2009.
(33) Lenz, A.; Ojamae, L. *Chem. Phys. Lett.* **2006**, *418*, 361−367.
(34) Manas, E. S.; Xu, Z. B.; Unwalla, R. J.; Somers, W. S. *Structure* **2004**, *12*, 2197−2207.
(35) Bruning, J. B.; Parent, A. A.; Gil, G.; Zhao, M.; Nowak, J.; Pace, M. C.; Smith, C. L.; Afonine, P. V.; Adams, P. D.; Katzenellenbogen, J. A.; Nettles, K. W. *Nat. Chem. Biol.* **2010**, *6*, 837−843.
(36) Cances, E.; Mennucci, B.; Tomasi, J. *J. Chem. Phys.* **1997**, *107*, 3032−3041.
(37) Mennucci, B.; Tomasi, J. *J. Chem. Phys.* **1997**, *106*, 5151−5158.
(38) Mennucci, B.; Cances, E.; Tomasi, J. *J. Phys. Chem. B* **1997**, *101*, 10506−10517.
(39) Tomasi, J.; Mennucci, B.; Cances, E. *J. Mol. Struct.: THEOCHEM* **1999**, *464*, 211−226.
(40) Jorgensen, W. L.; Chandrasekhar, J.; Madura, J. D.; Impey, R. W.; Klein, M. L. *J. Chem. Phys.* **1983**, *79*, 926−935.
(41) Krieger, E.; Darden, T.; Nabuurs, S. B.; Finkelstein, A.; Vriend, G. *Proteins: Struct., Funct., Bioinf.* **2004**, *57*, 678−683.
(42) Duan, Y.; Wu, C.; Chowdhury, S.; Lee, M. C.; Xiong, G.; Zhang, W.; Yang, R.; Cieplak, P.; Luo, R.; Lee, T.; Caldwell, J.; Wang, J.; Kollman, P. *J. Comput. Chem.* **2003**, *24*, 1999−2012.
(43) Wang, J.; Wolf, R. M.; Caldwell, J. W.; Kollman, P. A.; Case, D. A. *J. Comput. Chem.* **2004**, *25*, 1157−1174.
(44) Krieger, E.; Nielsen, J. E.; Spronk, C. A.; Vriend, G. *J. Mol. Graphics Modell.* **2006**, *25*, 481−486.
(45) Kwok, K. C.; Cheung, N. H. *Anal. Chem.* **2010**, *82*, 3819−3825.
(46) Lawson, D. M.; Haisenleder, D. J.; Marshall, J. C. *Life Sci.* **1993**, *53*, 1267−1272.
(47) Jiang, Q.; Payton-Stewart, F.; Elliott, S.; Driver, J.; Rhodes, L. V.; Zhang, Q.; Zheng, S.; Bhatnagar, D.; Boue, S. M.; Collins-Burow, B. M.; et al. *J. Med. Chem.* **2010**, *53*, 6153−6163.
(48) Ratna, W. N. *Life Sci.* **2002**, *71*, 865−877.
(49) Loprinzi, C. L.; Zahasky, K. M.; Sloan, J. A.; Novotny, P. J.; Quella, S. K. *Clin. Breast Cancer* **2000**, *1*, 52−56.
(50) Jordan, V. C. *J. Med. Chem.* **2003**, *46*, 1081−1111.